Final Report
NAG5-8614 Period Covered: 07/01/1999-06/30/2003

Application of Satellite SAR Imagery in Mapping the Active Layer of Arctic Permafrost

Shusun Li, V. Romanovsky, Joe Lovick, Z. Wang, and Rorik Peterson

Geophysical Institute,
903 Koyukuk Drive, PO Box 757320
University of Alaska Fairbanks
Fairbanks, AK 99775-7320
Phone: (907) 474-7676
Fax: (907) 474-7290
E-mail:sli@asf.alaska.edu

1. Introduction

A method of mapping the active layer of Arctic permafrost using a combination of conventional synthetic aperture radar (SAR) backscatter and more sophisticated interferometric SAR (INSAR) techniques is proposed. The proposed research is based on the sensitivity of radar backscatter to the freeze and thaw status of the surface soil, and the sensitivity of INSAR techniques to centimeter- to sub-centimeter-level surface differential deformation. The former capability of SAR is investigated for deriving the timing and duration of the thaw period for surface soil of the active layer over permafrost. The latter is investigated for the feasibility of quantitative measurement of frost heaving and thaw settlement of the active layer during the freezing and thawing processes. The resulting knowledge contributes to remote sensing mapping of the active layer dynamics and Arctic land surface hydrology.

2. Objectives

The proposed work consists of (1) determining the onset dates of surface soil thawing and freezing and the length of the thaw season of the active layer, (2) feasibility study of mapping surface differential deformation using INSAR techniques, and validating the patterns generated from SAR imagery via field measurements at various sites over the proposed study area if the method is feasible, and (3) mapping large scale variations of permafrost in a study area along the Dalton Highway between Fairbanks and Prudhoe Bay, Alaska.

3. Implementation and Results

3.1. Field Experiment

1. Three new permafrost observation sites were established and equipped with Campbell data loggers, air and ground surface temperature probes, MRC

temperature probes (temperature sensors at 11 depths) and Vitel soil moisture probes (three depths):

Toolik Lake, 68°37'23.2''N; 149°36'36.4''W , Elevation: 756 m
Sagwon MAT, 69°25'32.6" N, 148°41'34.8"W , Elevation: 300 m
Sagwon MNT, 69°25'59.8" N, 148°40'12.3"W , Elevation: 290 m

All data from these new sites have been collected every hour during 2000-2003. These data are prepared for submission to the National Snow and Ice Data Center (NSIDC).

2. Air and ground surface temperatures and active layer and near-surface permafrost temperatures (every three hours) and soil moisture data (daily) for 1999-2003 were collected from existing permafrost observation sites (West Dock, Deadhorse, Franklin Bluffs, Galbraith Lake).

3. Frost-heave and thaw settlement monitoring instrument (Figure 1) was developed and installed at West Dock (one set), Deadhorse (three sets), Franklin Bluff (two sets), Sagwon MAT (two sets), and Sagwon MNT (two sets). Measurements of the total frost heave at these sites during the cold seasons 2000-2001, 2001-2002, and 2002-2003 were performed.

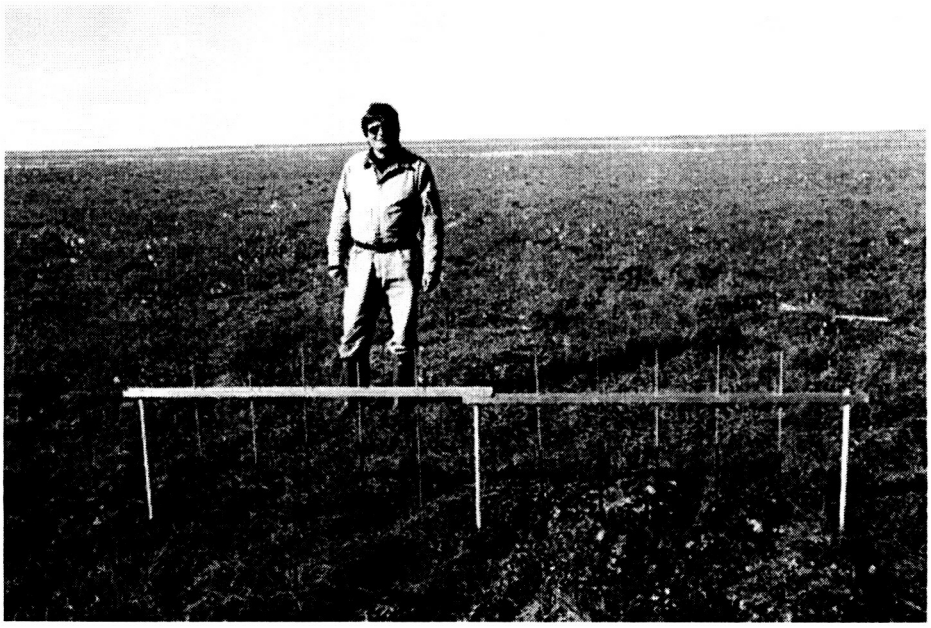

Figure 1. Heavometer in field.

3.2. Determining the onset dates of surface soil thawing and freezing and duration of thaw season

3.2.1. Use of Archived SAR images

We produced time series of SAR images using images archived at the Alaska SAR Facility (ASF) to capture the radar backscatter change in relation with the soil freeze and thaw status. Fig. 2 is the L-band backscatter change with the annual freeze and thaw cycle captured by the JERS-1 SAR images. The series also reveals the transition from freeze to thaw to the south of Franklin Bluffs (the location outlined by blue box) on June 2-3, 1997. A time series of ERS-1 SAR images acquired in late 1999 (Fig. 3) provide information of the onset of winter freezing at Franklin Bluffs in that year. The greatest ERS SAR back scatter decrease occurred between September 11 and 27, which implies that freezing occurred between those two dates.

All these examples suggest that time series of ERS and JERS SAR images are useful to capture transitions between soil surface freeze and thaw status. Identification of exact dates of onset of surface soil freezing and thawing is possible at places where transitional zone between thaw areas of high backscatter and freeze areas of low backscatters is visible along satellite SAR image swaths.

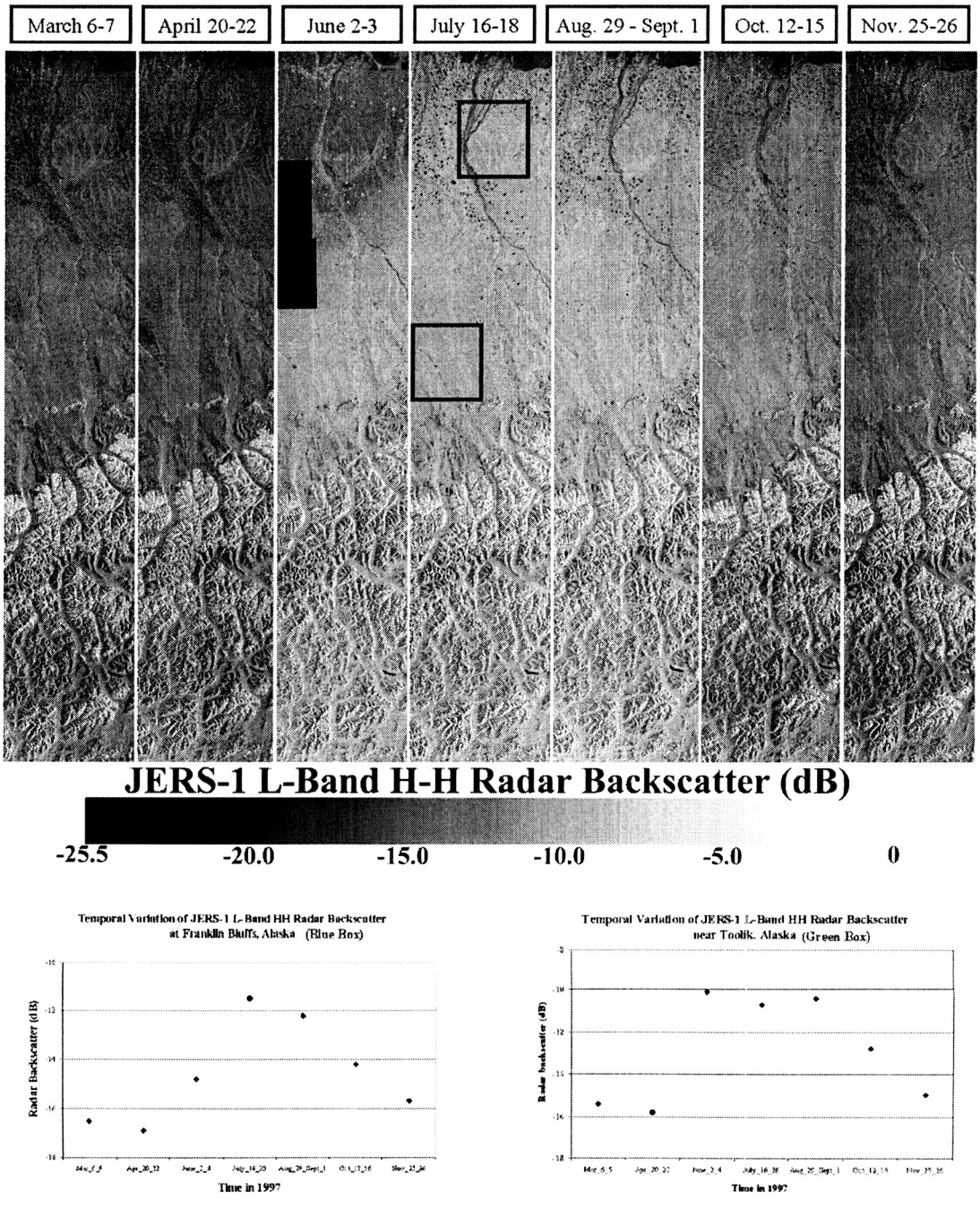

Fig.2 Time series of JERS-1 SAR images acquired in 1997 reveals the L-band radar backscatter change with annual freeze and thaw cycle.

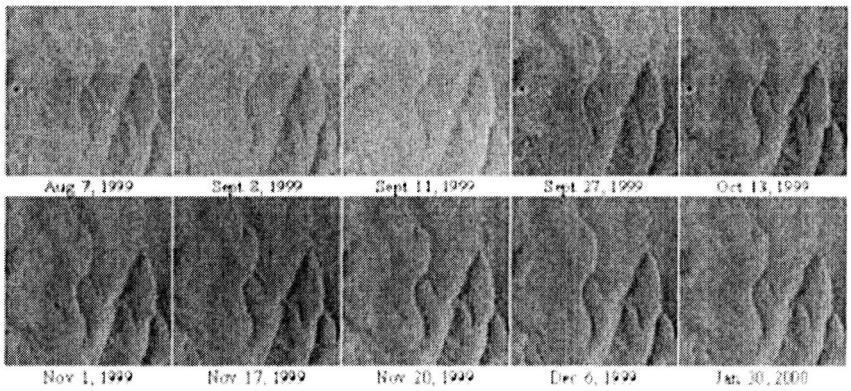

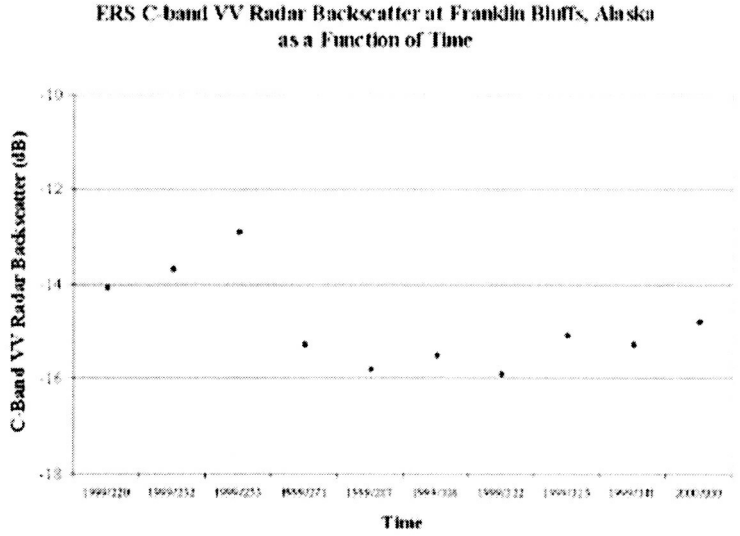

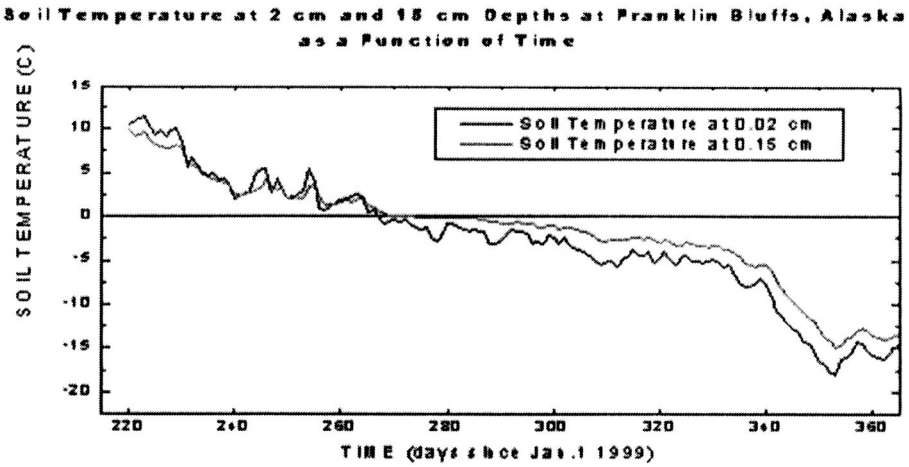

Fig. 3 Time series of ERS-1 SAR images indicates that soil was freezing around September 27, 1999 at Franklin Bluffs where a transitional zone is visible.

3.2.2. Use of RADARSAT SAR images acquired during the field campaign

During the field campaign in 2000, we collected time series of concurrent RADARSAT SAR images. We use a combination of eight images from Standard beam 7 to study a systematic variation in backscatter with respect to the season and other factors. Colour composite images, formed using subsequent scenes stacked into the RGB channels, have the effect of colouring the changes, making the variation easier to distinguish. The six resultant colour images are seen in Figure 4. The change in overall hue, from blue to cyan to grey to yellow to red, is expect as lower intensity images occur in the early and late parts of the year, when the ground is frozen.

Figure 5 further provides the details of the systematic change of backscatter of different types of ground cover from scene to scene, as a result of the annual temperature cycle (Figure 6).

The winter scenes have a significantly lower backscatter than the scenes acquired when temperatures were above freezing. This can be clearly seen in Figures 4A and 5A, in which the ground was frozen in all three scenes. In Figures 4B and 5B, the ground was frozen in the first two component scenes, but thawed in the third one, resulting a strong blue hue. The lakes are yellow (red + green) in A and just red in B, because in April and May lakes were covered with cold lake ice, which has high backscatter, but they were covered by floating lake ice with melting snow on top by the 22nd of May, which exhibits low radar backscatter. Figures 4C and 5C show approximately uniform brightness of thawed soil in all three component-scenes, giving a grey overall colouring. In Figures 4D and 5D, the brightness of the scenes from August are strongest, probably due to the increase in backscatter from vegetation.

The scenes from late in the year (Figures 4E, 4F, 5E, and 5F) strongly illustrate the lower backscatter of images after freeze-up, with E having a yellow hue, indicating little input from the 20th September Image and in F, strong red hue showing continued low backscatter values in the October image.

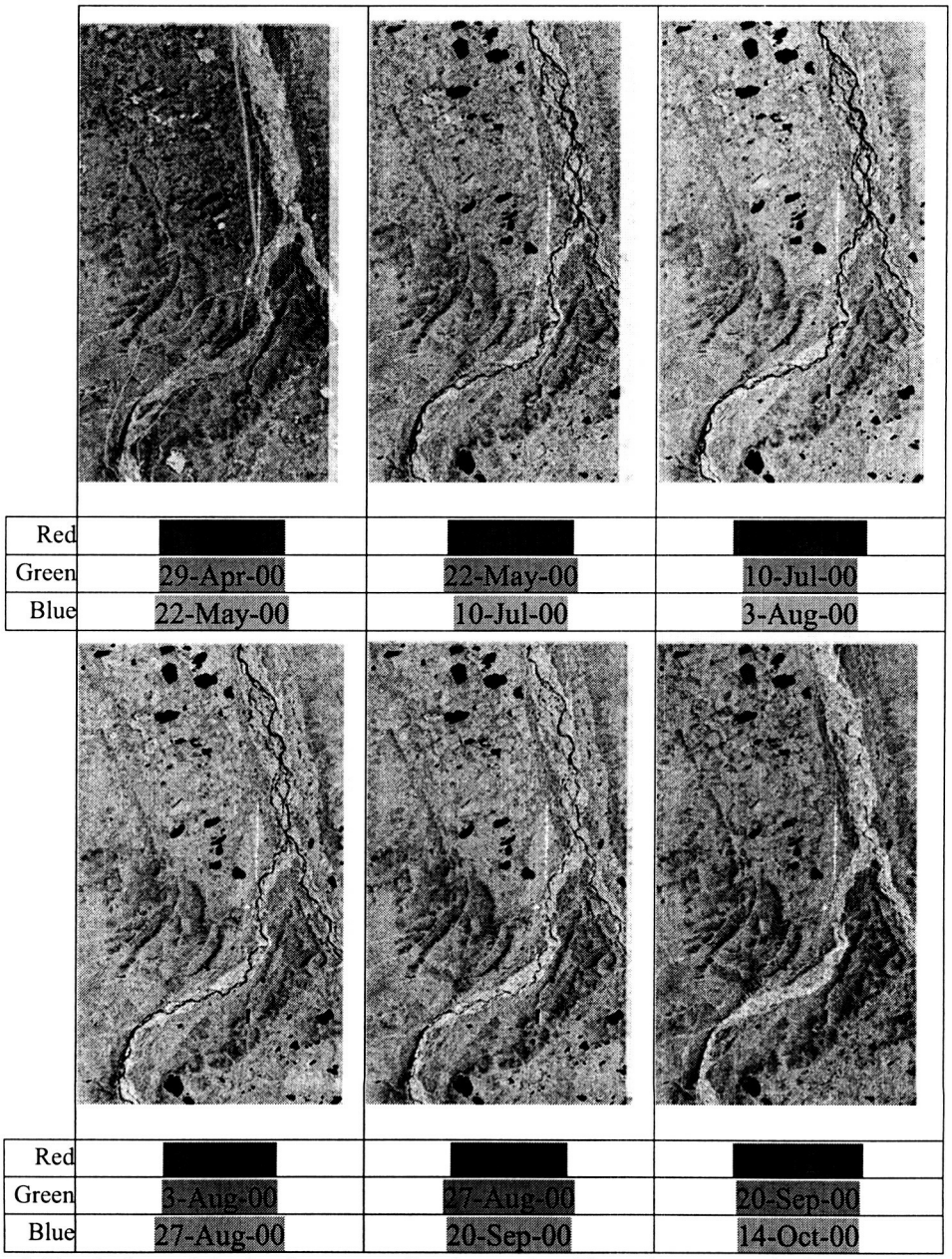

Figure 4, Evolution of the backscatter of artic tundra. The winter months have a lower backscatter return on average (images 1,6 being darker). In (A) the May image (blue) dominates colouring the whole scene, giving it a blue tinge and the bottom right image (F), has a strong August channel (Red), and a corresponding red tinge.

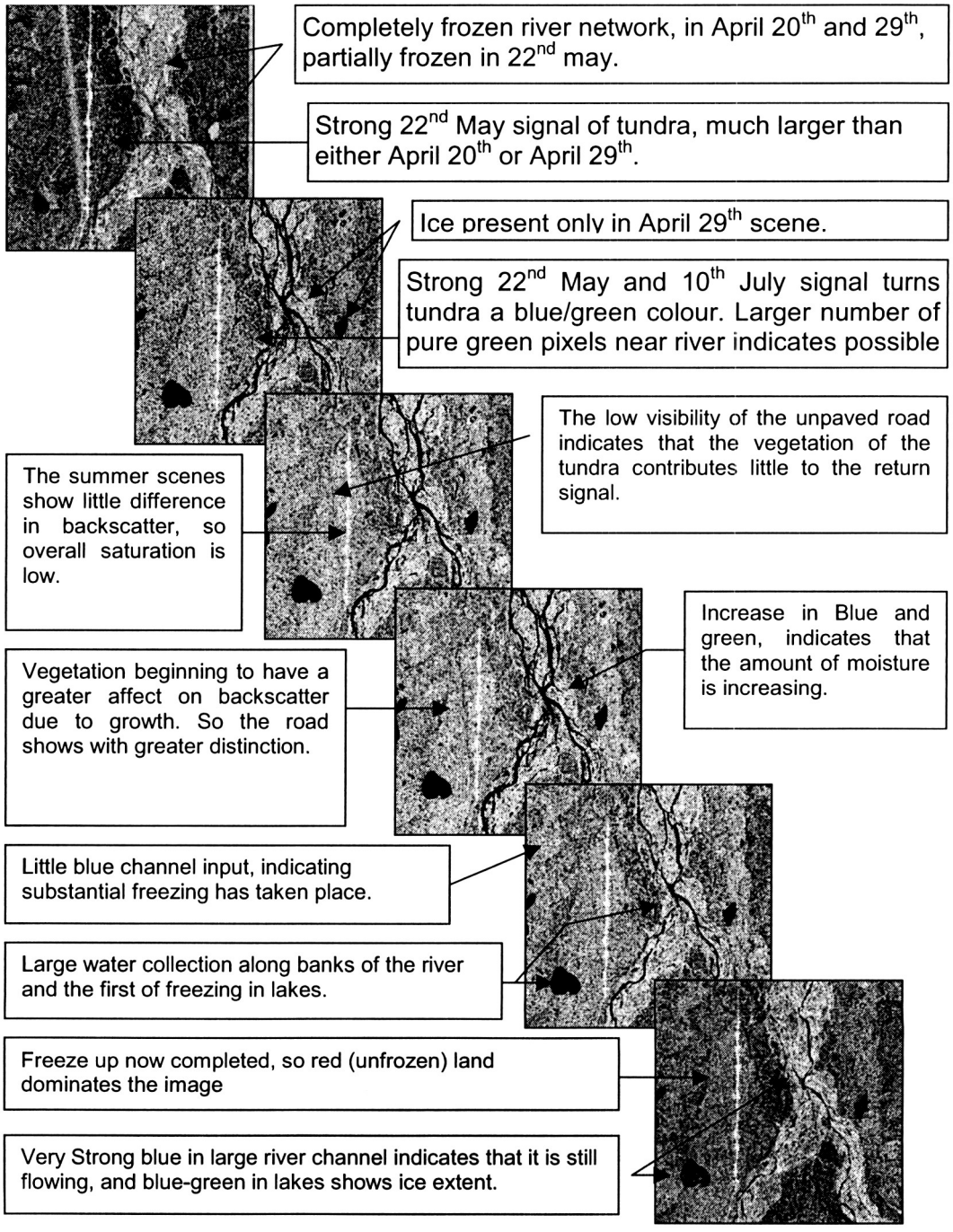

Figure 5, Details of how backscatter changes for different ground cover over time, and the strong effects of moisture, freezing and vegetation change.

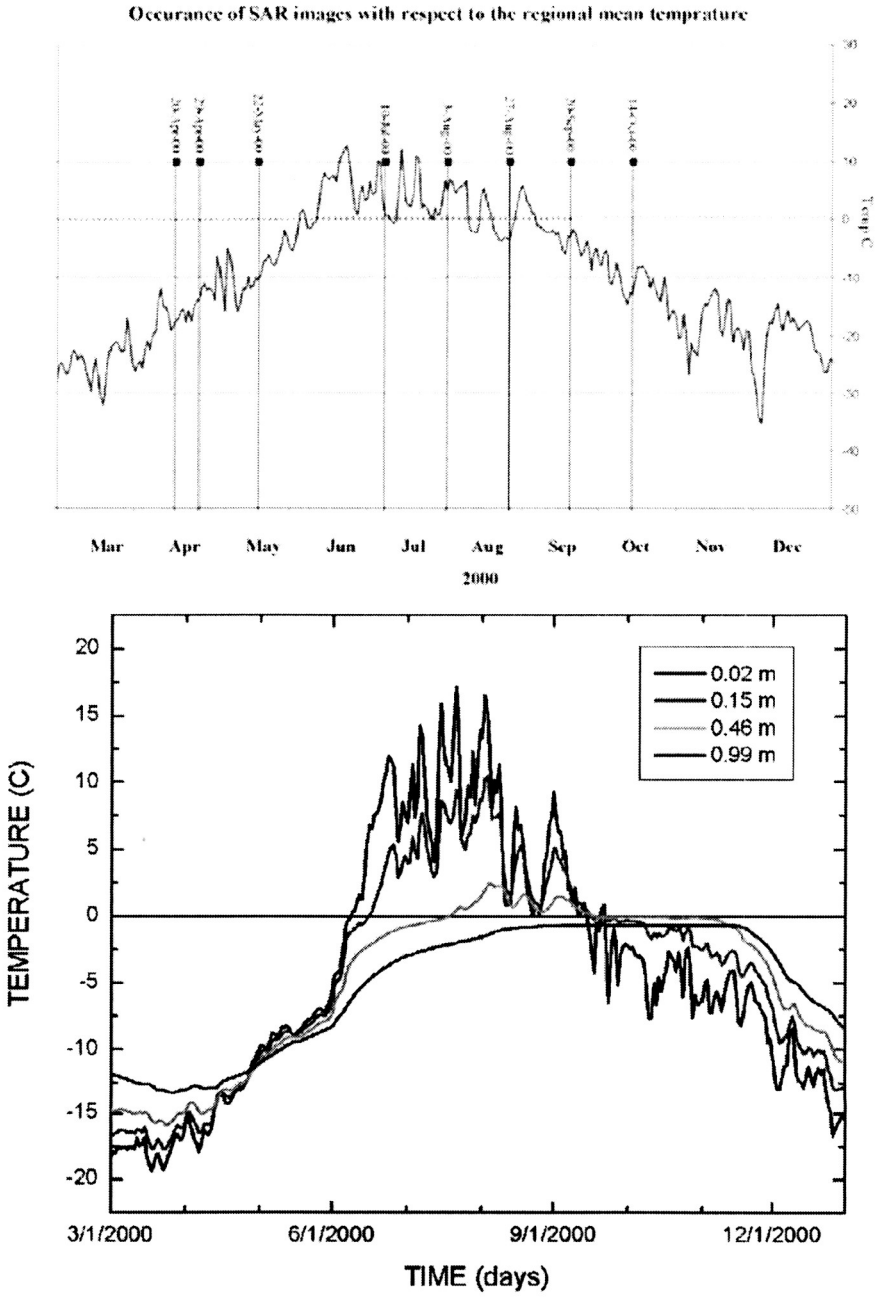

Figure 6. Occurrence of SAR images in Figure 4 and 5 with respect to annual temperature cycle.

3.3. Quantification of Frost Heave and Thaw Settlement Using InSAR Techniques

We generated a 35-day interferogram at Toolik, Alaska. The interferogram is constructed from SAR images acquired on August 30 and October 4, 1995, respectively (Fig. 7a). The corresponding backscatter image is in Figure 7b. Terrain effects on fringes in the interferograms have been removed using another interferogram made from a pair of ERS-1 and -2 SAR images acquired on 4 and 5 October 1995, respectively (Fig. 7c). The resulting interferogram (Fig. 7d) basically shows a pattern of differential surface deformation. In the resulting interferogram, less subsidence (or equivalently, more up-heaving) is seen at the tops of the hills and along the river channels than at the surrounding areas. The difference in surface deformation was about 1 cm. Interpretation of the resulting pattern is not straightforward. A numerical simulation of the soil thermal regime using weather data does not indicate substantial freezing in soil by the end of the period (Fig. 8). Therefore, the differential surface deformation seen on the interferogram is not likely caused by differential frost heave. These results probably could be explained by continuous thawing of the active layer during unusually warm September of 1995. Because of this thawing, the related settlement of the ground surface was observed within the landscapes with increased amount of ice in the upper permafrost layer. Our research shows that for this region the active layer continues to thaw as long as temperature at the ground surface stays above +2C (Romanovsky and Osterkamp, 1997). During the period of discussion, the daily mean surface temperature stayed mostly above +4C. The ice content in the lower part of the active layer is much larger on slopes compare to relatively dry hilltops and gravely channels sediments. Our data from direct measurements of the temperature field dynamics at the Franklin Bluff site shows continues thawing during September 1995 that resulted in the one of the deepest active layer during the entire period of measurements (1986-2003). This supports suggested above explanation.

In the study area, we made a great effort to generate interferograms from all available ERS-1, ERS-2 and RADARSAT SAR images. However, we are not able to produce decent interferograms for the freezing and thawing periods, from which we can make sensible interpretation of quantitative estimation of frost heave and thaw settlement.

The field measurements (Figure 9) obtained between mid-August 2000 and mid-August 2001 suggest that frost heave and thaw settlement not only show variations on large scales, but also exhibit heterogeneous variations with scales as small as sub-meters. The latter poses some difficulties to InSAR investigation because heterogeneous variation of frost heave and thaw settlement tends to reduce the coherence and increase the noise of the interferograms. Frequent melt and refreezing of snow cover, increase or decrease of snow water equivalent, and change of soil surface freeze and thaw status during the transitional periods cause significant change in spatial distribution of radar backscatterers in individual SAR pixels. All these factors contribute to the difficulty in producing decent interferograms for quantifying frost heave and thaw settlement in the study area.

Frost heave is generally small at the coastal sites because at some sites the thickness of the active layer was only 0.3 m West Dock). At other sites (Howe Island) with deeper active layer, the soil water content was relatively low and the texture of soils was much coarser than within the inland sites. Between inland sites, the sites with non-acidic type of

vegetation (much less moss at the ground surface) show much larger frost heave (Deadhorse, Franklin Bluffs, and SagMNT sites) than the sites with acidic type of vegetation (SagMAT and Happy Valley sites). This fact stresses the importance of vegetation type and abundance for the frost heave process that was not appreciated in the past.

While we have not been successful in extracting quantitative estimates of frost heave and thaw settlement from interferogram, we were able to use interferometric coherence map to delineate different types of local-scale variability in the frost heave and different types of tundra in the area. The mapping is important because the difference in vegetation and exchange of C02, methane, and other trace gases between different tundra types is significant. Example of such a mapping will be given in section 3.4.

(a)

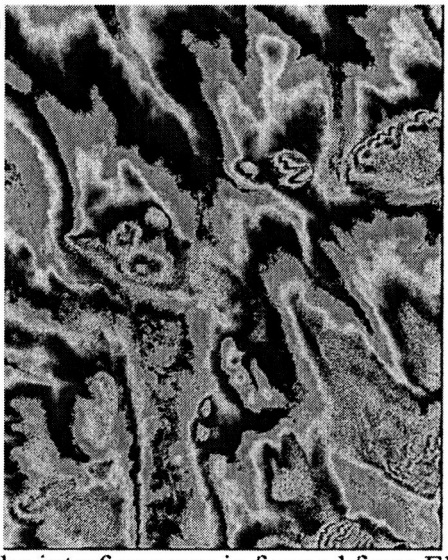

The interferogram is formed from ERS SAR images acquired on August 30 and October 4, 1995. The satellite baseline was 54m.

(b)

ERS SAR amplitude image.

(c)

The interferogram is formed from ERS SAR images acquired on 4 and 5 October 1995. The orbital baseline is 221 meters.

(d)

Deformation pattern is formed from ERS SAR images acquired on August 30 and October 4, 1995. The terrain effects have been removed.

Fig. 7 (a) An interferogram constructed from a pair of SAR images acquired on August 30 and October 4, 1995. The SAR backscatter is shown in (b). The terrain effects have been removed using (c). The resulting interferogram (d) shows surface differential deformation pattern. The image size is 40 by 50 km.

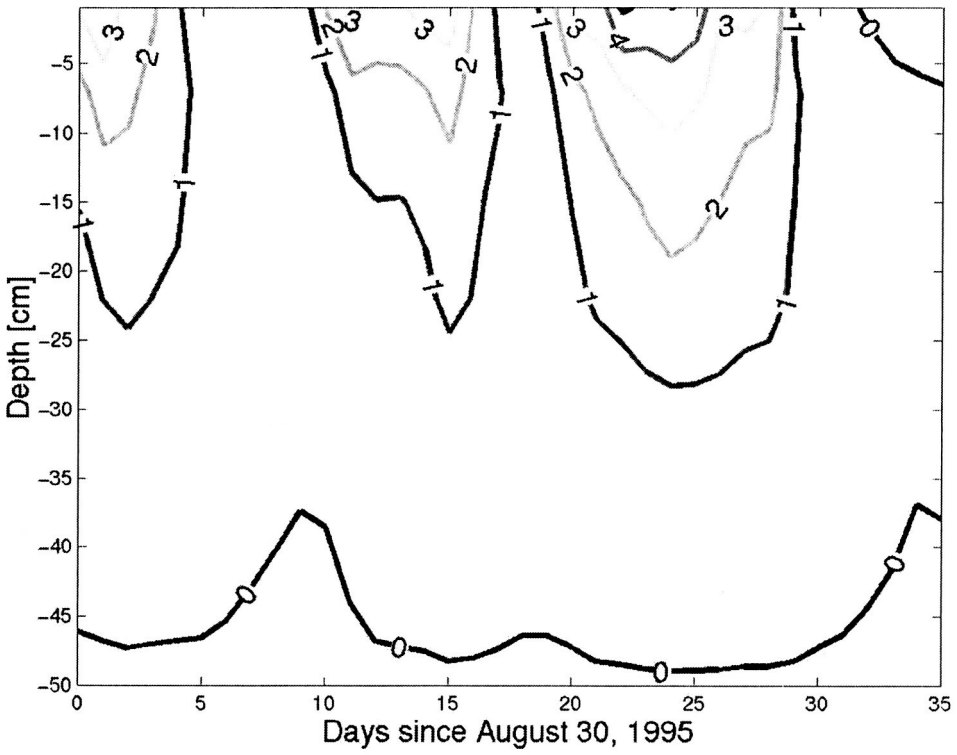

Fig. 8 The active layer thermal regime for Happy Valley area , Alaska, simulated from weather data.

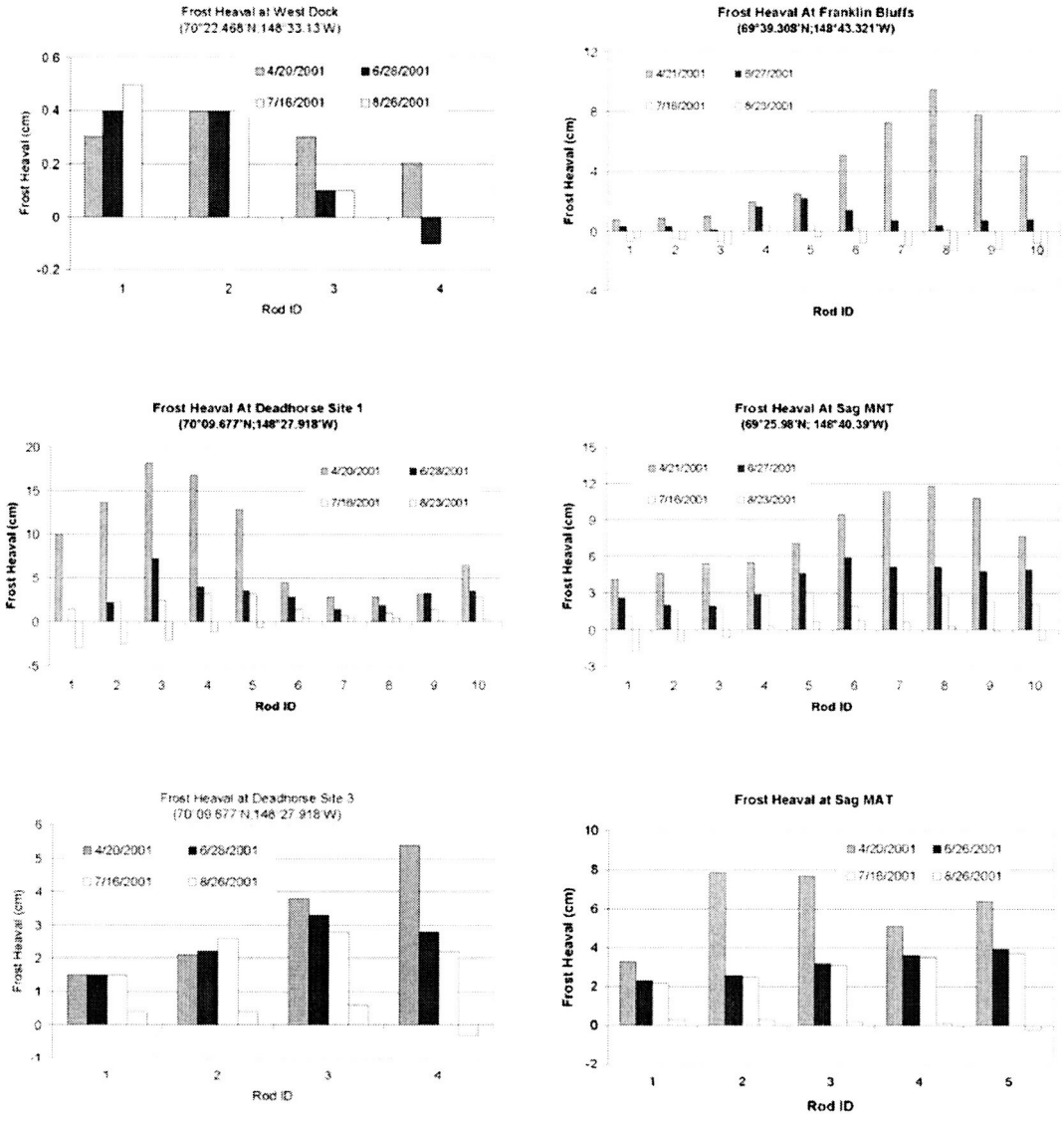

Figure 9. Frost heave and thaw settlement measured in 2001. All the readings are relative to mid-August (16-18 August) 2000.

3.4. Mapping Different Tundra types in the Study Area

We used the principal component analysis method to derive principal component images from time series of RADARSAT SAR images. We found that a set of principal component images can be used to delineate the boundary between the moist acidic tundra (MAT) and moist non-acidic tundra. Figure 10 compares the boundaries derived from the RADARSAT beam modes 5, 6, and 7, with the boundaries from MODIS, and the Landsat-based map of the area. The agreement among them is good.

We were able to produce interferometric coherence maps that provide a good delineation of the MAT/MNT boundary (Figure 11), although not all coherence maps can be used for the same purpose. An interferometric coherence map is useful for this study only when other factors, such as weather, snow melt and storm, dramatic soil moisture change, transition between soil surface freeze and thaw status, do not exert a strong impact on the interferogram.

The interferometric coherence map shown in Figure 11 was derived from a pair of RADARSAT SAR images acquired on 17 August and 10 September 2000, respective.

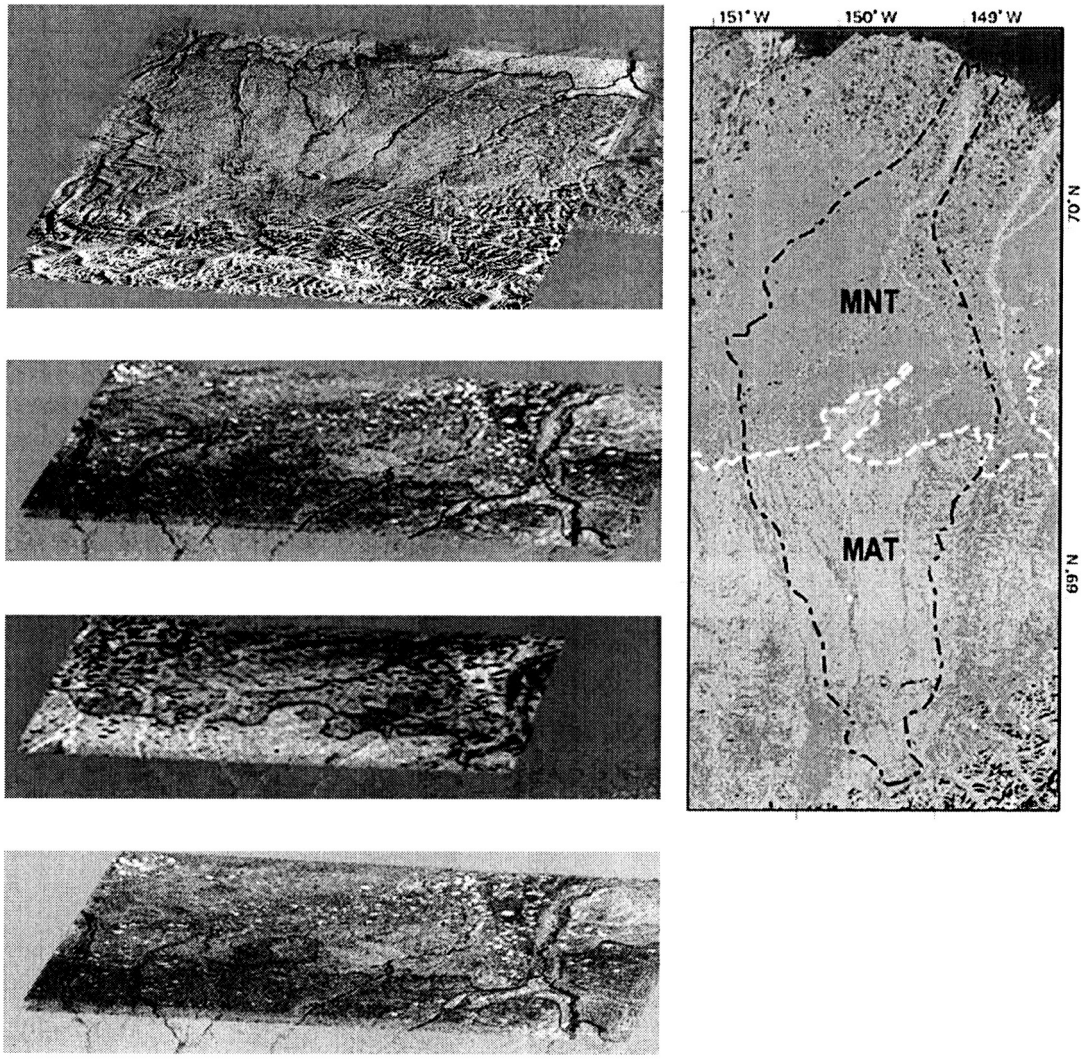

Figure 10, Principal component images derived from time series of Radarsat beam modes (a) 5,(b) 6, (c) 7 SAR images, and (d) a false color MODIS image, respectively, each showing the boundary between MNT (above red line) and MAT (bellow red line) tundra. To the right is a map of the Kuparuk basin with the same boundary shown as a white dashed line (from Walker et al., 1988).

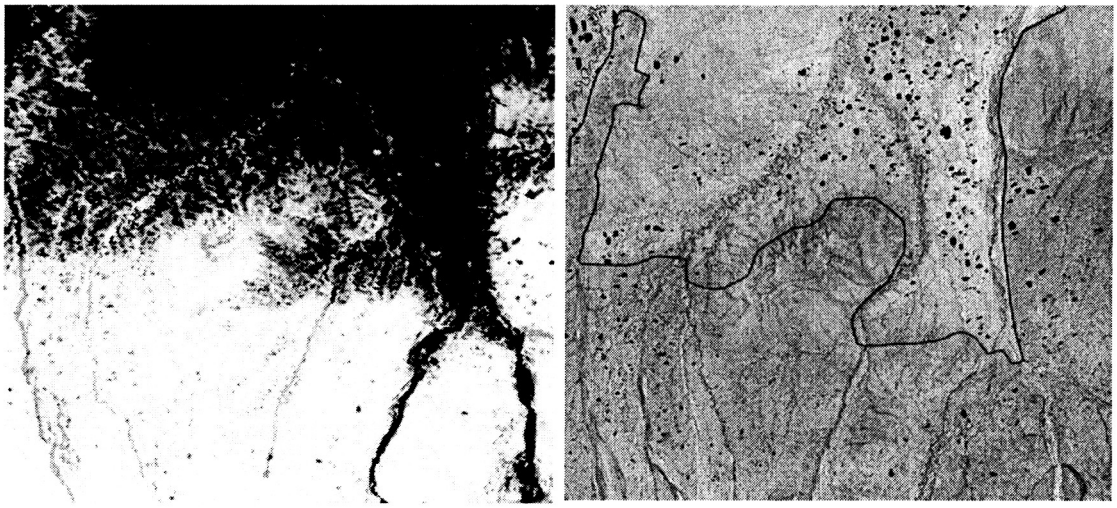

Figure 11. Comparison of MNT and MAT delineation from (a) An NDVI image generated from a MODIS 250 m resolution scene of 17th July 2002, and (b) an interfeormetric Coherence image from RADARSAT beam mode 6 SAR images acquired on 08-17-2000 and 09-10-2000. The boundary is between MNT and MAT is highlighted, MAT to the South (bottom).

3.5. Other related findings

3.5.1. Wind-drift snow

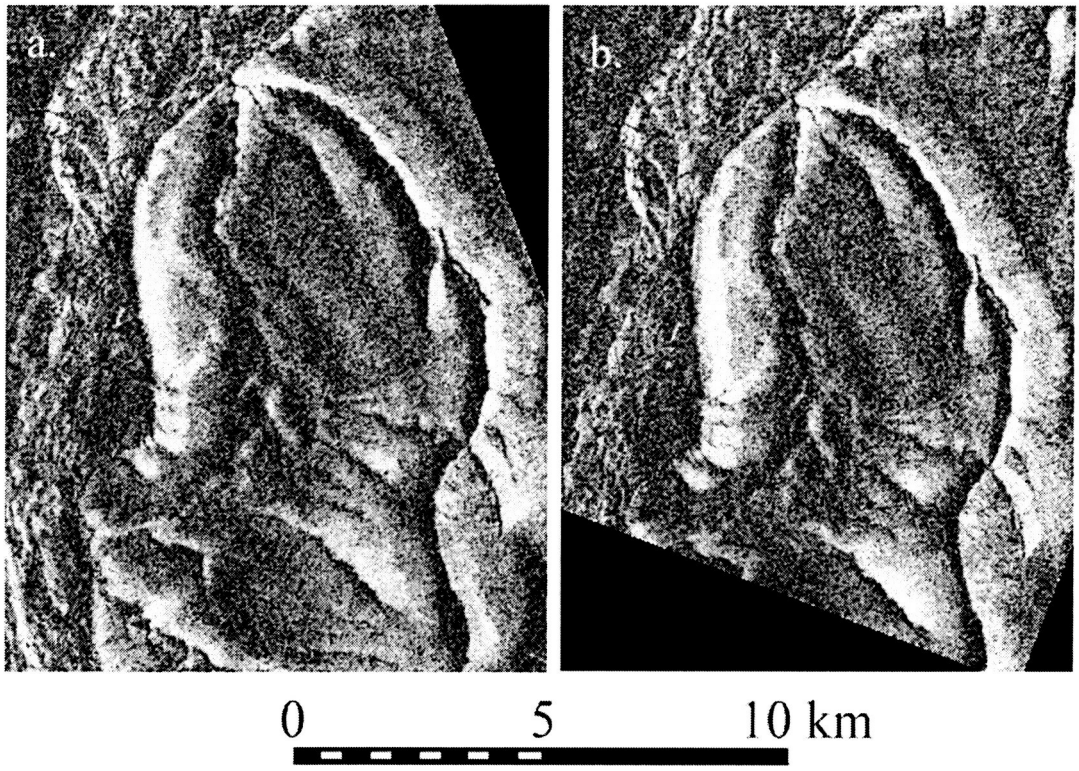

Figure 12. Examples of coherence images in time series for the Franklin Bluffs site. The Bluff is the rougher topography in the SE (lower right) part of the images. The time intervals involved in the interferogram generations are (a) 13 - 16 February from east looking orbits; and (b) 12 - 15 February from west looking orbits.

During the InSAR investigation, we found that it is possible to use InSAR techniques to study redistribution of snow on the terrain by wind drift. Although snow is not the main focus of this investigation, the strong impact of snow on ground thermal regime makes the investigation of snow a legitimate issue in permafrost study. We use the SAR images acquired during the second ice phase (from late December 1993 to early April 1994) of the first European Remote Sensing Satellite (ERS-1) when the satellite repeated its orbits every three days. Such a temporal pattern is ideal for study subtle temporal changes. On 5 February, based on the sonic sounders, about 7 cm of snow fell on the region. Between 10 and 15 February, however, persistent strong westerly winds with speeds reaching 12 m s^{-1} swept the area. For this period, the coherence maps show a distribution pattern of alternating light and dark strips that are strongly correlated with topography and aspect with respect to the wind. The patterns cannot be explained by artifacts caused by radar and terrain interactions; identical patterns are seen on all east looking interferograms derived

from ascending satellite passes (Figure 12a) and also on the one available west-looking interferogram derived from descending passes (Figure 12b). As an example, around Franklin Bluffs, high coherence was observed on west-facing slopes while low coherence was observed on east-facing slopes, though the subtle details of the snow distribution are more complicated. We interpret these patterns to be widespread areas of windward scour and leeward deposition. To our knowledge, the coherence maps are the first time that such patterns have been "visualized" in this detail over such a large scale.

3.5.2. Model Simulation of Polarimetry SAR response to freeze and thaw status of soils

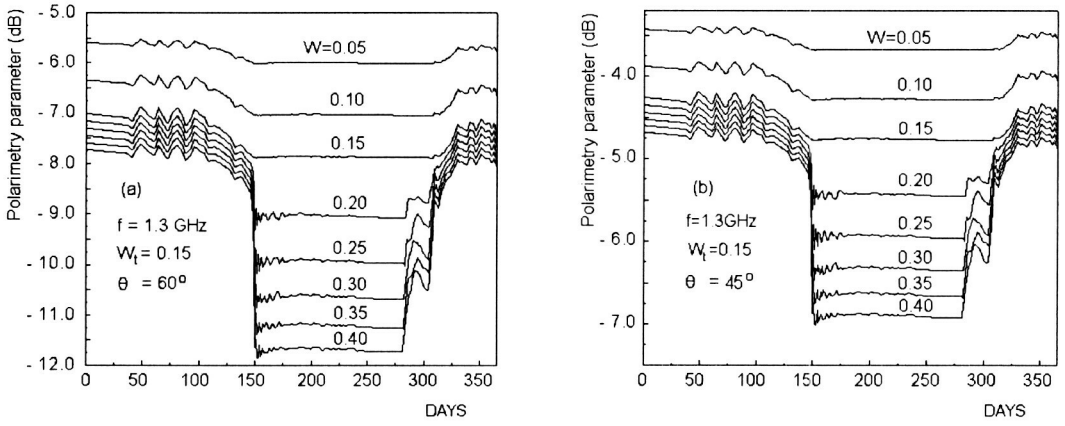

Figure 13. Seasonal variations in the polarimetric parameter related to annual temperature cycle with the soil volumetric moisture W being a parameter, calculated at two incidence angles (a) $\theta = 60^{\circ}$, and (b) $\theta = 45^{\circ}$.

We collaborate with Dr. V. L. Minorov at Siberian Branch of the Russian Academy of Sciences, and Dr. Altai State University to investigate the response of polarimetric SAR to freeze and thaw status of soils. Based on the generalized refractive mixing dielectric model, the soil complex dielectric constant (CDC) profiles are derived as a function of soil temperature with soil moisture as a parameter for representative soils. The soil temperature profiles with depth in the active layer of permafrost are input into the model using measurement at some test sites in Alaska [V.E. Romanovsky, T.E. Osterkamp, 1997]. Once the soil CDC profile and radar incidence angle are known, the proportion of the statistically averaged HH to the VV backscatter (BBP) can be modeled through solving the Maxwell equations in the small perturbation method approximation. The simulated BBP is sensitive to the status of soil freeze and thaw status as is shown in Fig. 13.

4. Education

Mr. Joe Lovick received M.S. degree at Department of Geology and Geophysics, University of Alaska Fairbanks, May 2003

Publications

- Li, S, and M. Sturm, Pattern of wind-drifted snow on the Alaskan arctic slope, detected with ERS-1 interferometric SAR, Journal of Glaciology, 48(163), 495-504, 2002.
- Li, S., Polar Environments Assessment by Remote Sensing, R.A. Meyers (Ed.) Encyclopedia of Analytical Chemistry, John Wiley & Sons Ltd, Chichester, 8660-8679, 2000.
- Wang, Z., and S. Li, Phase unwrapping through a Branch-cut-based cut-bridging and window-patching method, *Applied Optics*, 38(5), 805-814, 1999.
- Paetzold, R. F., Hinkel, K. M., Nelson, F. E., Osterkamp, T. E., Ping, C. L., and V. E. Romanovsky, Temperature and Thermal Properties of Alaskan Soils, in *Advances in Soil Science*: Global climate change and cold regions ecosystems/ edited by R. Lal, J. M. Kimble, B. A. Stewart, Lewis Publishers, pp. 223-245, 2000.
- Romanovsky, V. E., and T. E. Osterkamp, Effects of unfrozen water on heat and mass transport processes in the active layer and permafrost, *Permafrost and Periglacial Processes*, 11, 219-239, 2000.
- Romanovsky, V. E. and Osterkamp, T. E., Permafrost Monitoring System in Alaska: Structure and Results (in Russian), *Earth Cryosphere*, Vol. V, No. 4, 59-68, 2001.
- Romanovsky, V. E., and Osterkamp, T. E., Permafrost: Changes and Impacts, in: R. Paepe and V. Melnikov (eds.), "Permafrost Response on Economic Development, Environmental Security and Natural Resources", *Kluwer Academic Publishers*, 297-315, 2001.
- Walker, D. A., H. E. Epstein, W. A. Gould, A. Kade, A.M. Kelley, J. A. Knudson, W. B. Krantz, R. A. Peterson, G. Michaelson, R.A. Peterson, C. L. Ping, M. A. Raynolds, and V. E. Romanovsky, Y. Shur, M.D. Walker, Biocomplexity of frost-boil ecosystems: a conceptual model of frost boil development in relationship to vegetation along a bioclimate gradient, *Permafrost and Periglacial Processes*, in review.

- Komarov, S. A., V. L. Mironov, and S. Li, SAR Polarimetry for Permafrost Active Layer Freeze/Thaw Processes, IEEE 2002 International Geoscience and Remote Sensing Symposium, Toronto, Ontario Canada, 24-28, June 2002, p.2654-2656, 2002.
- Lovick, J. and S. Li, Fusion of Radarsat SAR interferograms with Other Image and Geological Data Sets to Establish Temporal, Spatial and Physical behaviors of the Active Layer at Sagwon, Alaska, AGU 2002 Fall Meeting, *Eos Trans. Suppl. 83*(47), p. F261, 2002
- Lovick, J., S. Li, and V. Romanovsky, Interpretation of RADARSAT SAR interferograms of Sagwon, Alaska, to establish temporal and physical permafrost parameters, EOS, suppl. *82*(47), p. 551, 2001.
- Wang, Z., and S. Li, Detection of Winter Frost Heaving of the Active Layer of Arctiv Permafrost Using SAR Differential Interferograms, *Proceedings of IEEE 1999 International Geoscience and Remote Sensing Symposium 1999* (IGARSS'99), 28 June – 2 July, 1999, Hamburg, Germany, 1946-1948, 1999.
- Wang, Z., and S. Li, Detection of Thaw Settlement of the Active Layer over Permafrost Near Toolik Lake, Alaska, During Early Summer Using DINSAR Technique, 50th Arctic Science Conference, 19-22 September 1999, Denali National Park, p.116, 1999.
- Romanovsky, V. E. and T. E. Osterkamp. Unfrozen Water in the Active Layer and Permafrost and Its Effects on Physical and Biological Processes, *EOS*, Trans. AGU, 80(46), F33, 1999.
- Wang, Z., and S. Li, Thaw Deformation of Permafrost Active Layer Near Toolik Lake, Alaska, Imaged by DINSAR Technique During Summer Time, AGU, 1999 Fall Meeting, EOS, Transactions, AGU, 80(46), F413, 1999.

Thesis

Lovick, J., Interpretation of Radarsat SAR scenes of Sagwon Alaska, to establish temporal, spatial and physical active layer behavior, MS thesis, Department of Geology and Geophysics, University of Alaska Fairbanks, May 2003, 88p, 2003.